Int J Adv Manuf Technol (2015) 77:565–572
DOI 10.1007/s00170-014-6464-5

ORIGINAL ARTICLE

Inclusions in steel: micro–macro modelling approach to analyse the effects of inclusions on the properties of steel

Akash Gupta · Sharad Goyal · K. A. Padmanabhan · A. K. Singh

Received: 26 February 2014 / Accepted: 2 October 2014 / Published online: 21 October 2014

Abstract The performance requirements of steel sheets are becoming increasingly stringent. Inclusions present as non-metallic phases affect the mechanical properties and workability in the down-stream processes of the sheet production adversely. By knowing how the inclusions affect the properties, suitable process parameters can be identified to avoid the defects formation during the forming operations. A very small size of the inclusions necessitates their behavioural study at the micro-scale. This requires a micro–macro modelling approach to identify the effects of the inclusions on forming operations such as hot rolling. In this work, a comprehensive micro–macro model is presented to quantify the effects of the inclusions and their characteristics on the properties of steel during solidification and forming. A micro-model developed using 2-D Finite Element Method is used to study void formation and its evolution at the inclusion/matrix interface (interfacial damage) and stress evolution in and around the inclusions. The model is then employed to study the effects of inclusion properties (hard/soft), its size and shape on the properties of the steel matrix. The constitutive equation for the macro-scale simulation of hot rolling is updated based on the findings of the micro-model. The modified constitutive equation at the macro-scale will allow the choice of a suitable process-parameters regime that will avoid failure during hot rolling and also lead to improved final properties in steel containing inclusions.

A. Gupta · S. Goyal · K. A. Padmanabhan · A. K. Singh (✉)
TRDDC–TCS Innovation Labs, Tata Consultancy Services Ltd., 54 B, Hadapsar Industrial Estate, Pune, Maharashtra 411013, India
e-mail: amarendra.singh@tcs.com

K. A. Padmanabhan
School of Engineering Sciences & Technology, University of Hyderabad, Hyderabad 500046, India

Keywords Micro–macro modelling · Steel · Inclusion · Constitutive equation · Mathematical modelling

1 Introduction

Consumers continue to place increasingly stringent demands on the quality and performance of steel sheets. Microstructure, macrostructure, segregation and cleanliness, which are the major concerns, play an important role in determining the properties of steel sheets and their performance during the applications. Among these, cleanliness is a major concern for steel manufacturers. For large-scale industrial production at competitive costs, it is not possible to provide steel with very high cleanliness level. Therefore, control of non-metallic inclusions in steels is critically important for ensuring high performance [1–5].

Non-metallic inclusions, for example, oxides and sulphides, form during the processing of the liquid steel and embed in the matrix during solidification. Distribution of inclusions in the matrix, along with their composition, morphology, size and relative strength, plays an important role in determining the effects of inclusions on the performance of the steel. Inclusions disrupt the homogeneity of the structure and affect various surface and bulk mechanical properties (for example, strength, drawability, brittle fracture, fracture toughness, hardness, corrosion and fatigue strength) both during the processing as well as in the final finished product [5]. During subsequent deformation processing, such as rolling, forging, stamping, and so on, inclusions could act as sites of stress concentration and lead to cracks and deteriorate fatigue strength. Debonding, sliding and separation may occur at the inclusion/matrix interface during the deformation processing [1–4].

Eshelby [6, 7] studied the elastic field in and around an ellipsoidal inclusion in a matrix. He concluded that the strain

inside the inclusion is uniform. Finite Element Method (FEM) is widely used for the analysis of the inclusion–matrix system. It has been used to study void formation and crack initiation at the inclusion–matrix interface during hot rolling [1, 2, 8, 9] and cold rolling [3, 10]. The latter authors have concluded that during rolling, inclusions that are harder than the matrix leads to void formation, whereas the softer inclusions elongate, as is evident from Fig. 1 [8]. Evolution of the stress field around an inclusion was studied in [4, 11, 12]. Stiénon et al. [4] used nano-indentation to characterise the mechanical properties of the inclusions. Gupta et al. [13] studied through a micro-mechanical approach the strategies for inclusion removal during the liquid steel processing and the effect of the inclusion on the deformation field around it through micro-mechanical approach.

Inclusions present in steel are in the micron size range. However, they can have a significant effect on the macro-scale properties during processing. Therefore, modelling at micro-scale is required to understand the behaviour of the inclusions in a steel matrix. Modelling of the inclusion–steel matrix interface is a big challenge since it is very difficult to determine the interface properties accurately using experiments. In published literature, authors have used a number of techniques to model the interface, such as (a) coherent interface [4, 11], (b) incoherent interface with Coulomb Friction [4, 8, 10] and (c) Cohesive Zone Model (CZM) [1, 14]. Modelling with coherent interface or with the friction model is an easy choice, but it may not provide a good insight into the behaviour of the inclusion–matrix system. Parameters for the CZM of the interface have been estimated in literature [15] using experiments, coupled with a numerical method for polymer-coated steel (using a peel-off test), fibre-reinforced metal matrix composite (using a push-out test) and so on. In these cases, the interface properties could be determined, but determining the inclusion–matrix interface properties experimentally is very challenging.

Micro-model along with one of the methods of incorporating interface properties can elucidate the effects of inclusions on the steel matrix at the micro-scale. However, industrial processes also have to be modelled at the macro-scale. Inclusions on a micro-scale and process conditions on a macro-scale together affect the final product properties. Therefore, it is necessary to model both the effects simultaneously. One method could be the use of very fine mesh, of the order of a micron, which is of the same length scale as that of the inclusions. Such an approach will require enormous computing time for solving even a single case and may not be useful in identifying the suitable process parameters. A sub-modelling approach, in which boundary conditions for the micro-model are set from an analysis of the macro-model, is an alternative. However, it will also be computationally expensive.

The objective of the present work is to provide a computationally efficient methodology for linkage of micro-scale and macro-scale models. In this approach following earlier suggestions [1, 8, 10, 11], initially a micro-model for the inclusion–matrix system is built. This micro-model is then used to identify the change in the material model of an equivalent homogenous material. The equivalent material model of the homogeneous material thus obtained is then used in the macro-model to obtain suitable process parameters. The next sections in this paper describe the micro-model, parametric studies with the micro-model and a methodology for obtaining the equivalent homogenous material model.

2 Micro-model: inclusion in steel matrix

The micro-model simulates the inclusion behaviour in the steel matrix. Plane strain behaviour is assumed. A two-dimensional (2-D) FEM-based micro-mechanical model is developed to analyse stress distribution in the inclusion–matrix system as well as the behaviour of the interface, that is, void formation at the interface of inclusion and matrix, which is experimentally observed in the case of hard inclusions present in steel matrix (refer to Fig. 1a).

2.1 Finite element equations

The formulations used in this model are based on the principle of virtual work. The governing equation for the static mechanics problem is given by force equilibrium equation

$$\sigma_{ij,j} + f_i^B = 0 \tag{1}$$

where ,σ_{ij} denotes stress tensor components and f_i^B is the component of body force. The finite element equation, which follows from principle of virtual work, is given by

$$\int_V \sigma_{ij}\delta e_{ij}\mathrm{d}V = \int_V f_i^B \delta u_i \mathrm{d}V + \int_S f_i^S \delta u_i \,\mathrm{d}S \tag{2}$$

where f_i^S is the external force acting on the surfaces of the body. Material constitutive model is used to represent the relation between stress and strain increment [16].

2.2 Constitutive model

To apply the micro-model to simulate the hot rolling conditions, simulation studies are executed at different temperatures and strain rates for different inclusion volume fractions. Inclusions are considered to be spherical and hard (Al_2O_3) with elastic–plastic properties (bilinear isotropic hardening) given in Table 1 [17]. Tangent modulus is considered as 10 % of

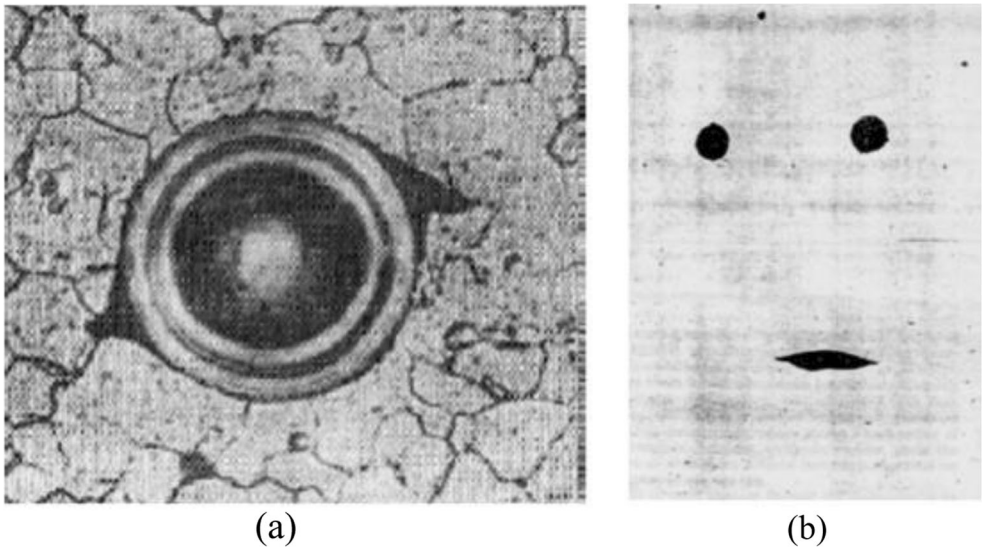

Fig. 1 Inclusions embedded in a steel matrix: **a** void formation due to a hard inclusion after a reduction of 50 %, **b** elongation of soft inclusion after a reduction of 42 % [8]

Young's modulus at a given temperature. Steel matrix is also considered to be elastic–plastic with power law hardening behaviour. The flow stresses for steel matrix were prescribed as [18]

$$\sigma_S = \alpha \exp\left(\frac{5000}{T}\right)\varepsilon^{0.23}\left(0.276\dot{\varepsilon}\right)^{\frac{0.133(T-273)}{1000}} \quad (3)$$

where $\alpha = 3.37 \times 10^6$

2.3 Model for the inclusion–steel interface

Computing interface properties for the inclusion–steel system experimentally is a challenge due to the very small size and low volume fractions of the inclusions. Indentation experiments or first-principle calculations [19] can be performed to get the interface properties. However, much success has not been achieved yet. Delamination of contact elements is referred to as debonding. In [20], interfacial debonding between the matrix and the primary and the secondary inclusion particles are modelled using decohesion potentials computed through quantum mechanics calculations, together with a mechanical model of normal separation and gliding induced dislocation.

Table 1 Inclusion properties as a function of temperature used in this model

Temperature (°C)	Young's modulus (GPa)	Yield strength (MPa)
800	353.1	246.1
1,000	330.0	241.4
1,200	320.0	137.9
1,400	225.5	29.7

In this paper, the CZM and Coulomb friction are used to simulate interface behaviour. The bilinear cohesive zone material model with mixed-mode debonding proposed by Alfano et al. [21] is used to characterise the constitutive behaviour of the interface. The interfacial separation is defined in terms of contact gap or penetration and tangential slip distance. In mixed-mode debonding, the interface separation depends on both normal and tangential components [16]. However, the CZM model has to be used carefully and its limitations are given in [15]. The CZM model consists of a constitutive relation between the traction T acting on the interface and the corresponding interfacial separation δ (displacement jump across the interface). For mixed-mode debonding, both normal and tangential contact stresses contribute to the total fracture energy and debonding occurs when the fracture energy reaches a critical level. Therefore, a power-law-based energy criterion is used to define the completion of debonding [16]

$$\left(\frac{G_n}{G_{cn}}\right)^2 + \left(\frac{G_t}{G_{ct}}\right)^2 = 1 \quad (4)$$

where G_n and G_t are normal and tangential fracture energies and G_{cn} and G_{ct} are their critical values. Obtaining the parameters for the CZM model is a challenge. In the absence of experimental data, shear component of mixed mode debonding is not considered whereas the values of the parameters assumed for the normal component are debonding stress $\sigma_{max} = 10^5$ Pa, debonding displacement $u = 10^{-6}$ m. Coefficient of friction was taken as 0.5 [1]. Complete debonding occurs when the debonding parameter (d_n) reaches a value of 1 [16].

2.4 Micro-model development

The model is developed using the commercial software ANSYS. 2-D, four-node structural solid element is used to

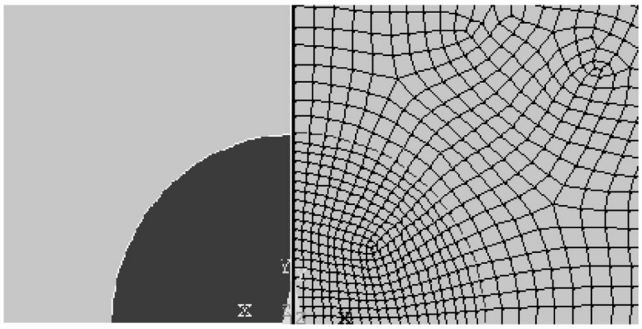

Fig. 2 Typical mesh generated in this study for the micro-model involving inclusion (dark phase) and steel matrix (light phase)

describe the inclusion and the steel matrix in a plane strain compression/tension test. Figure 2 shows a typical mesh of the micro-model involving the inclusion and the steel matrix. Each simulation is performed at a fixed temperature and strain rate for a particular inclusion volume fraction by changing the inclusion size. The inclusion/matrix interface is considered as a weak interface, the details of which are given in Section 2.3. Inclusion–matrix interface is modelled using 2-D, two-node surface-to-surface contact element at inclusion surface and 2-D target element at corresponding steel matrix surface. It is assumed that the interface is initially bonded and it debonds on applying a certain amount of tensile/shear load. After debonding, friction resists the sliding at the interface. Figure 3a and b shows the results from simulations for hard and soft inclusion, respectively. Figure 3a shows the contour plot of equivalent stress around a hard circular inclusion embedded in a steel matrix with void being formed at the interface during a plane strain compression test. This result is similar to that of Fig. 1a. Similarly, Fig. 3b shows the contour plot of equivalent stress around a soft circular inclusion embedded in the steel matrix during a plane strain compression test. In case of soft inclusion, there is no void formation at the interface and the inclusion elongates, which is similar to what is shown in Fig. 1b. Thus, the model results are qualitatively matching the experimental results found in published literature [8].

2.5 Validation of the micro-model

Yang et al. [11] simulated the steel–inclusion system by assuming a coherent interface for the inclusion harder than steel as well as the inclusion softer than steel. They analysed a number of inclusion geometries, namely, circular, square, rhombus and trapezium, as well as inclusions of different sizes. Elastic behaviour for both inclusion and steel matrix was assumed. Figure 4 shows the validation of micro-model developed in this study for the case of a hard square inclusion embedded in the steel matrix. Figure 4a shows the contour plot of equivalent stress for this case and Fig. 4b presents a comparison of the equivalent stress profile along line PQ of Fig. 4a, as predicted by the present model and Yang et al. [11]. Figure 5 compares the peak stress for different geometries of the inclusions (circle, rhombus, square) and for varying degrees of relative hardness of the inclusion with respect to the steel matrix. It can be concluded that square and rhombus shape inclusions which have sharp edges leads to stress concentration resulting in higher value of stresses as compared with the circular shape. It is observed from Figs. 4 and 5 that the present model agrees well with the results of Yang et al. [11].

Luo [1] studied steel–inclusion system using a cell model to simulate compressive deformation of inclusion in an elastic–viscoplastic matrix. Debonding and friction at inclusion–steel matrix interface were taken into account. Figure 6 shows the results of the micro-model compared to Luo [1] for the case of hard circular inclusion in steel matrix. Two parameters quantifying the void formation at the interface defined by Luo [1] have been compared. First is the extent of separation along the inclusion–matrix interface, which is described by arc angle (2α) between two cusps of the void to the centre of inclusion. Second is normalised void width (w) given by W/R, where W

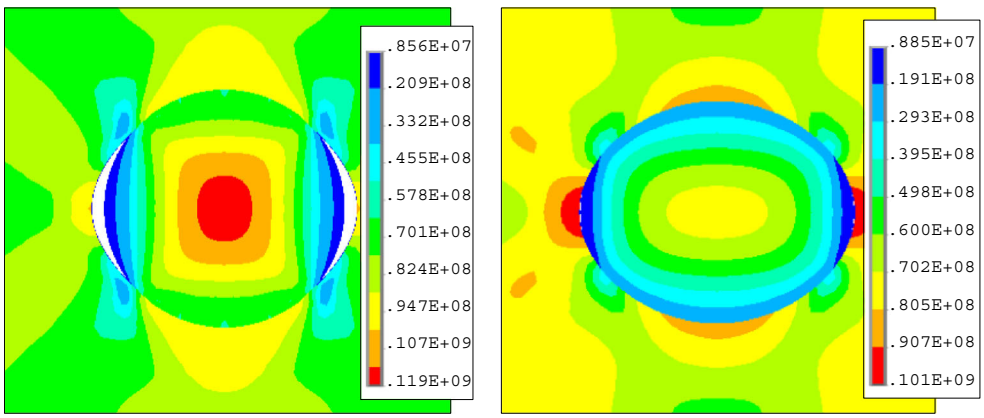

(a) (b)

Fig. 3 Example simulation results showing contour plot of equivalent stress around **a** hard and **b** soft, circular inclusion embedded in a steel matrix during plane strain compression test

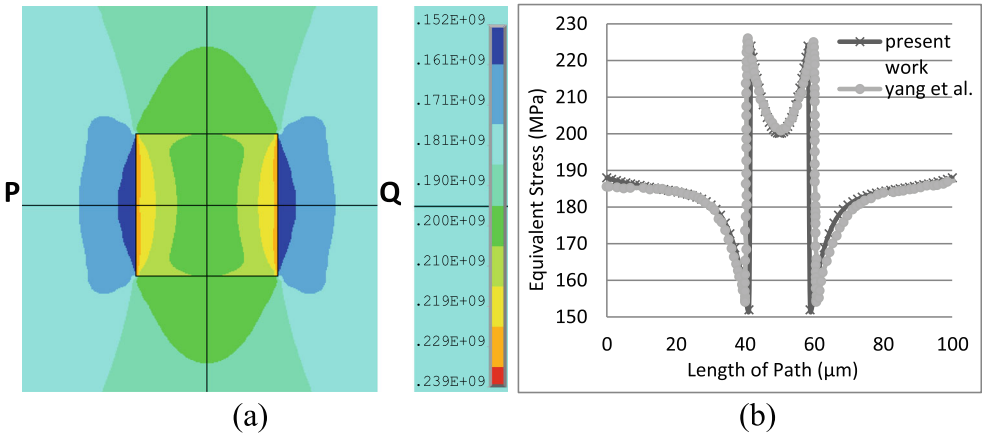

Fig. 4 **a** Contour plots of equivalent stress around a hard square inclusion embedded in steel matrix with coherent interface assumption, and **b** comparison of the equivalent stress along line PQ in (**a**)

is extent of horizontal separation between inclusion and matrix and R is inclusion radius [1]. 2α, W and R have been described in void schematic shown in Fig. 6a. Variation of these two parameters 2α and w with respect to the reduction in height of matrix has been plotted in Fig. 6b, and it can be observed that, as expected, 2α decreases and w increases with the increase in reduction percentage. Thus, it can be concluded that the present model also agrees well with the results of Luo [1].

3 Micro–macro modelling approach

The micro-model described in Section 2 is used to simulate plane strain compression tests at different temperatures, strain rates and inclusion volume fractions for hard spherical (Al_2O_3) inclusion. Steel matrix is assumed to occupy spatial dimensions of 100 μm × 100 μm. Inclusion volume fraction is varied from 0.0 to 0.2, with corresponding inclusion size variation of 0–25 μm. Temperature is varied from 800 to 1,400 °C and strain rate from 0.0001 to 0.1. The average (overall) true stress–strain response of the inclusion–steel matrix system is obtained from the micro-model simulations. This response for a temperature of 1,400 °C and strain rate of 0.01 s^{-1} is shown in Fig. 7 for inclusion volume of 0, 1 % and 3 %. Dataset consisting of 500 data points of stress–strain response are generated from different simulations of varying temperature, strain rate and inclusion volume fractions. Out of these, 400 are used to obtain an updated constitutive equation. The updated constitutive equation of equivalent homogenous material is obtained by non-linear regression using the generalised reduced gradient method [22]. The equation obtained from empirical fit is given as

$$\sigma_f = (1-V_i)^{2.88}\sigma_S \tag{5}$$

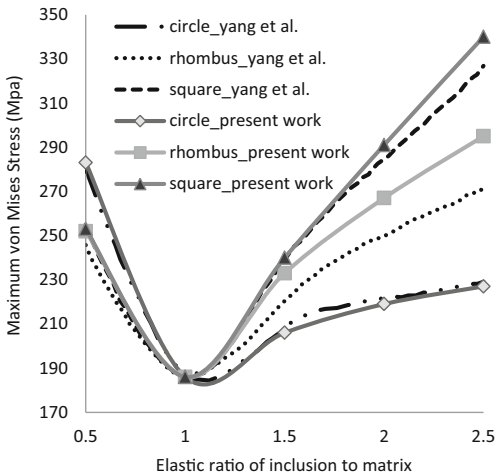

Fig. 5 Effect of different inclusion shapes and relative hardness with respect to steel matrix, on the peak stress

where σ_S is given by Eq. 3 and V_i is the inclusion volume fraction. In other words, an updated constitutive equation is obtained for the steel matrix with flow stress, as a function of inclusion volume fraction. The remaining 100 data points were used for validation of this equation. For each of the 100 data points, normalised error is calculated between value of stress obtained from simulation (actual) and the value of stress predicted using Eq. 5 (predicted) given as |actual−predicted|/actual. Mean $(\overline{E})$ and standard deviation (σ) of error is calculated for validation dataset and obtained values are $(\overline{E})$ =2.37 % and σ=1.84 %, indicating robustness of the developed fit. Figure 8 shows the variation of flow stress with inclusion volume fraction till a strain of 0.2 % is reached at three different temperatures. It can be observed that with an increase in the inclusion size (or the volume fraction of inclusions), force/stress required to deform the inclusion–steel matrix system to a given strain level decreases. Evidently, the load-bearing capacity of the material is reduced due to void formation in presence of inclusions. These results are consistent with results of Murakami [23] from which it can be

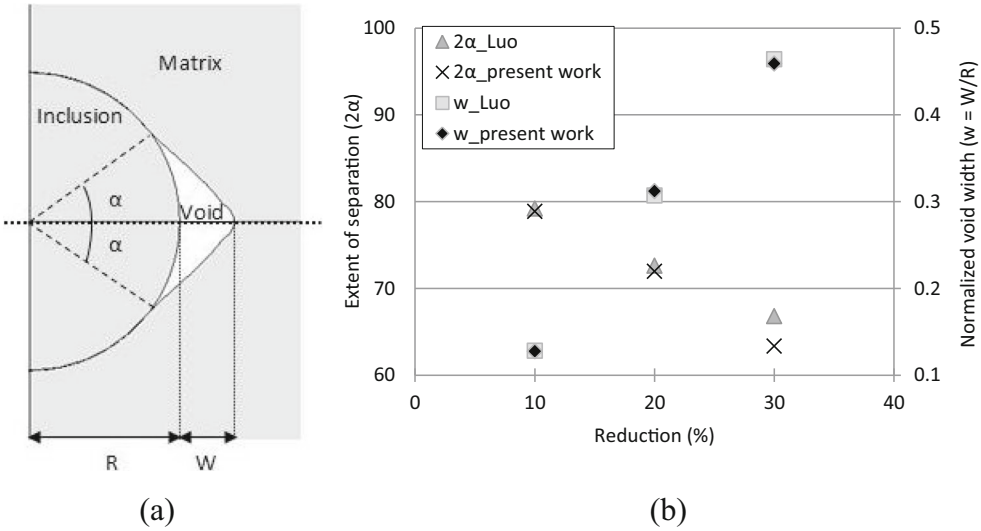

Fig. 6 **a** Schematic showing void and parameters related to it and **b** variation in extent of separation (2α) and normalised void width ($w=W/R$) with respect to reduction in height

concluded that the strength of material decreases with an increase in inclusion size.

4 Discussion

Micro–macro modelling approach is successfully applied for analysing the effects of inclusions on the properties of steel. Results of micro-model are validated and good qualitative match is obtained in the behaviour of hard and soft inclusions in comparison with what is reported in literature. The updated constitutive equation of the equivalent homogenous material is also developed and validated for the inclusion–matrix system using micro–macro modelling approach and practically useful good fit is obtained. This modified equation can be used as an updated material model to simulate the macroscopic process (for example, hot rolling) of inclusion–steel matrix system. Volume fraction of inclusions has to be specified at each element in mesh of steel matrix to use this modified material model for the system. It should be noted that the upstream process of continuous casting of steel results in an uneven distribution of inclusions in the steel slab cross-section. The above method of macro-scale simulation of the hot rolling process would be useful in two ways. Firstly, it will help to identify a set of process parameters so that the ill effects of the defects in the hot rolled steel sheet are minimised and the required properties are met. Secondly, when it proves impossible to obtain the steel sheet with required properties, it would help to identify the level of inclusions that can be tolerated during the processing (i.e. the inclusion level at which the stress predicted by the local updated constitutive equation falls below the permitted value. In turn, this depends on the inclusion level.) This restriction can then be posed to the slab supplier.

To explain this further, a simple case study was done. Two micro-model simulations of plane strain compression are performed with applied reduction of 6 %. Except inclusion size,

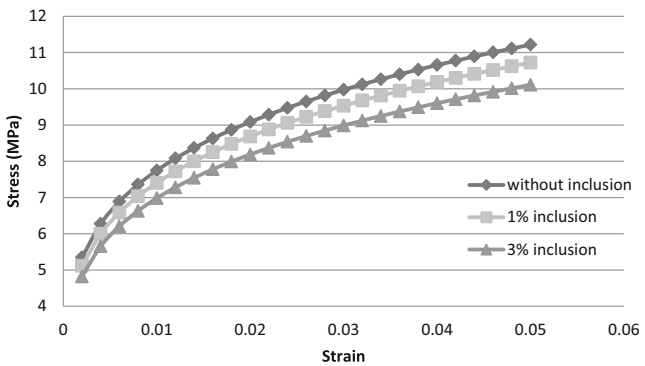

Fig. 7 Isothermal, iso-strain rate averaged stress–strain response of the inclusion–steel matrix system at T=1,400 °C and $\dot{\varepsilon}$ =0.01, as obtained from the micro-model simulation

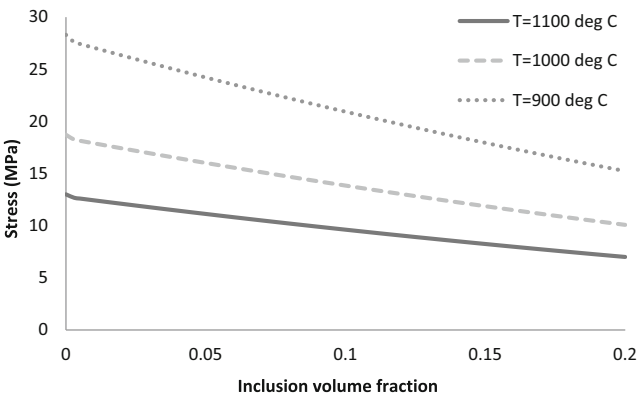

Fig. 8 Variation of flow stress (ε=0.002, $\dot{\varepsilon}$ =0.01 s^{-1}) with inclusion volume fraction at three different temperatures

all the other conditions are kept the same (temperature= 800 °C, strain rate=0.001 s^{-1}) in the two simulations. In the first case, inclusion size is 5.5 μm (volume fraction 0.01) and normalised void width (w) at the end of simulation is 0.007, while in the second case inclusion size is 25 μm (volume fraction 0.2) and w obtained is 0.008. It can be concluded that larger size inclusion results in higher void width. Thus, the macro-scale simulation of hot rolling performed using the method described above will help to identify what level of w or other similar parameters can be tolerated and accordingly limit on inclusion size can be identified. Zhang et al. [24] have reported typical steel cleanliness requirements which not only vary with steel grade but also with its end use. For example, automotive and deep drawing sheet can tolerate maximum inclusion size of 100 μm [24]. Therefore, identifying the level of inclusions using macro-scale simulation of hot rolling that can be tolerated in steel will depend on processing requirements and specific application.

It must be noted that tuning with the plant condition will be required for using Eq. 5. Experimental study will also be useful for validation of Eq. 5 as such an approach is not reported in the open literature. For experimental validation, physical simulations using a Gleeble machine can be performed on samples of the steel containing hard and soft inclusions. Torsion tests should be performed at different temperatures and strain rates to obtain modified flow curves as in the process of hot rolling, where the material behaviour changes because of the presence of inclusions.

5 Conclusions

A new methodology based on a micro–macro modelling approach is presented in this paper to quantify the micro-scale effects of inclusions on the macro-scale properties of the steel sheet. Based on the results presented in this paper, the following conclusions are made:

(a) The size, properties (hard or soft) and shape of inclusions have a strong effect on stress concentration and peak stress in a steel sheet in which inclusions are embedded.
(b) In case of hard inclusions, void formation takes place at inclusion–matrix interface when a weak interface is assumed. Contact gap formed at the interface increases with an increase in the size of the inclusion.
(c) In case of coherent interface, for hard inclusion, the peak stress occurs at the edge of the inclusion, while for soft inclusion, the peak stress occurs in the matrix. Inclusions with sharp edges such as square and rhombus shape leads to stress concentrations and higher values of stresses as compared with the circular shape.
(d) For hard circular inclusion with weak inclusion–matrix interface, the extent of separation decreases and void width increases, with an increase in the reduction in height of the matrix during compressive deformation.
(e) Flow stress decreases with increasing inclusion volume fraction, that is, load-bearing capacity of the material decreases due of the formation of voids at weak inclusion–matrix interface in case of spherical hard inclusions.
(f) Updated constitutive equation of the equivalent homogeneous material is obtained as a function of inclusion volume fraction. This could be used to select suitable process parameters for the simulation of macroscopic processes such as hot rolling, which in turn will help in process design using Integrated Computational Materials Engineering-based platforms such as TCS-PREMAP [25].

Acknowledgements Encouragement and support from TCS CTO, Mr K Ananth Krishnan, and TRDDC Process Engineering Lab Head, Dr Pradip, are gratefully acknowledged.

References

1. Luo C (2001) Evolution of voids close to an inclusion in hot deformation of metals. Comput Mater Sci 21:360–374
2. Luo C, Ståhlberg U (2001) Deformation of inclusions during hot rolling of steels. J Mater Process Technol 114:87–97
3. Yu HL, Bi HY, Liu XH, Tu YF (2008) Strain distribution of strips with spherical inclusion during cold rolling. Trans Nonferrous Metals Soc China 18:919–924
4. Stiénon A, Fazekasa A, Buffière JY, Vincent A, Daguier P, Merchi F (2009) A new methodology based on X-ray micro-tomography to estimate stress concentrations around inclusions in high strength steels. Mater Sci Eng A 513:376–383
5. Ghosh A (2001) Secondary steelmaking. CRC, Boca Raton
6. Eshelby JD (1957) The determination of the elastic field of an ellipsoidal inclusion and related problems. Proc R Soc Lond A Math Phys Sci. doi:10.1098/rspa.1957.0133
7. Eshelby JD (1959) The elastic field outside an ellipsoidal inclusion. Proc R Soc Lond A Math Phys Sci. doi:10.1098/rspa.1959.0173
8. Ervasti E, Stahlberg U (2005) Void initiation close to a macro-inclusion during single pass reductions in the hot rolling of steel slabs: a numerical study. J Mater Process Technol 170: 142–150
9. Hwang YM, Chen DC (2003) Analysis of the deformation mechanism of void generation and development around inclusions inside the sheet during sheet rolling processes. J Eng Manuf. doi:10.1243/095440503322617144
10. Yu HL, Bi HY, Liu XH, Chen LQ, Dong NN (2009) Behavior of inclusions with weak adhesion to strip matrix during rolling using FEM. J Mater Process Technol 209:4274–4280
11. Yang DX, Xie JP, Zhang KF, Liu ZF, Wang AQ (2009) Numerical simulation of stress field in inclusions of large rudder arm steel castings. China Foundry 6(3):219–225
12. Prasannavenkatesan R, Zhang J, McDowell DL, Olson GB, Jou HJ (2009) 3D modeling of subsurface fatigue crack nucleation potency of primary inclusions in heat treated and shot peened martensitic gear steels. Int J Fatigue 3:1176–1189
13. Gupta A, Kumar P, Anapagaddi R, Reddy N, Goyal S, Singh AK, Padmanabhan KA (2013) Integrated modeling of steel refining, casting and rolling operations to obtain design set points for quality

steel sheet production. NUMIFORM 2013, AIP Conf Proc. doi:10.1063/1.4806880
14. Allazadeh MR, Garcia CI, DeArdo AJ, Lovell MR (2009) Analysis of stress concentration around inclusions due to thermally induced strain to the steel matrix. JASTM Int. doi:10.1520/JAI102041
15. Siegmund T, Brocks W (1999) Prediction of the work of separation and implications to modeling. Int J Fract 99:97–116
16. ANSYS Release 14.0, Help System, Mechanical APDL, ANSYS, Inc
17. A MEMS Clearing house® and information portal for the MEMS and Nanotechnology community. http://www.memsnet.org/material/aluminumoxideal2o3bulk/. Accessed on 11 Feb 2013
18. Bernard G, Ribound PV, Urbain G (1981) Investigation of the plasticity of oxide inclusions. Rev Metall Cah Inf Tech 78:421–433
19. Dandekar CR, Shin YC (2011) Molecular dynamics based cohesive zone law for describing Al–SiC interface mechanics. Compos A: Appl Sci Manuf 42(4):355–363
20. Hao S, Liu WK, Moran B, Vernerey F, Olson GB (2004) Multi-scale constitutive model and computational framework for the design of ultra-high strength, high toughness steels. Comput Meth Appl Mech Eng 193:1865–1908
21. Alfano G, Crisfield MA (2001) Finite element interface models for the delamination analysis of laminated composites: mechanical and computational issues. Int J Numer Meth Eng. doi:10.1002/nme.93
22. Lasdon LS, Waren AD, Jain A, Ratner M (1978) Design and testing of a generalized reduced gradient code for nonlinear programming. ACM Trans Math Softw 4(1):34–50
23. Murakami Y (2002) Metal fatigue: effects of small defects and non-metallic inclusions. Elsevier, Amsterdam
24. Zhang L, Thomas BG (2003) State of the art in evaluation and control of steel cleanliness. ISIJ Int 43(3):271–291
25. Gautham BP, Singh AK, Ghaisas SS, Reddy SS, Mistree F (2013) PREMΛP—a platform for the realization of engineered materials and products. ICoRD'13, Lecture Notes in Mech. Eng., Chennai. doi:10.1007/978-81-322-1050-4_104